Luminance compensation in top-emitting organic light-emitting diodes with high color purity as quantum dots using horizontal dipole orientation

Hyunsu Cho [a],[*], Chan-mo Kang [a], Byoung-Hwa Kwon [a], Sukyung Choi [a], Chul Woong Joo [a], Hyunkoo Lee [a],[b]

[a] *Electronics and Telecommunications Research Institute (ETRI), Daejeon, 34129, Republic of Korea*
[b] *Department of Electronics Engineering, Sookmyung Women's University, Seoul, 04310, Republic of Korea*

ARTICLE INFO

ABSTRACT

Organic light-emitting diodes (OLEDs) and quantum dots (QDs) are mainstream applications in large-sized displays. Owing to their narrow photoluminescence (PL), QDs offer a wide color gamut. Although OLEDs have a wider PL spectrum bandwidth than that of QDs, a high color purity can be obtained through an optical design of the top-emitting device. However, the luminance improvement from the strong cavity effect in a top-emitting geometry is not significant because of the wide PL spectrum. This insufficient luminance improvement can be compensated by applying organic light-emitting materials with horizontally oriented dipoles. Luminance compensation is color dependent. In a blue light-emitting structure, the luminance improvement by a narrow PL spectrum is more advantageous than by a horizontal dipole orientation. However, in green and red light-emitting structures, even if the full width at half maximum of the PL is about 20-nm-wide, luminance can be compensated using a horizontal dipole orientation while maintaining high color purity.

1. Introduction

As display technologies continue to be developed, various characteristics of ultra-high-definition television have evolved to provide higher quality colors. The International Telecommunication Union (ITU)-R recommendation, more typically known as Rec.2020 or BT.2020, requires monochrome red, green, and blue primary colors (467, 532, and 630 nm) and has defined the widest color gamut [1,2]. This color gamut is extremely large, i.e., 72% larger than that of sRGB, and 37% larger than that of DCI-P3. The resulting color space contains 57.2% of the CIE 1976 chromaticity diagram. Currently, only a few displays can provide a color space similar to that of BT. 2020. To obtain primary colors that enable the optimization of the BT.2020 color gamut, it is more suitable to use a light-emitting material with a narrow photoluminescence (PL) spectrum to provide a wide color gamut. Consequently, the interest in quantum dots (QDs) has increased, and along with organic light-emitting diodes (OLEDs), they are now becoming a core technology in the display market.

Commercialized phosphorescent OLED materials are known to have a wide full width at half maximum (FWHM) of the PL spectrum, allowing them to be applied in next-generation lighting systems with a high color-rendering index [3,4]. To narrow the FWHM of the PL spectrum of organic light-emitting materials, Pt-based phosphorescent materials and new blue fluorescent materials have been investigated [5–10]. It is widely known that QD materials have a narrower FWHM of the PL spectra than both fluorescent and phosphorescent OLED materials. The FWHM of the PL spectrum differs depending on the type of QDs: the PL spectra of the InP- and Cd-based QDs have FWHMs of approximately 40 and 30 nm, respectively [11–21]. Moreover, many studies on perovskite materials, the PL spectra of which exhibit an FWHM of 20–30 nm, have been recently published [22–26]. The FWHM of the PL spectra of various emitting materials is summarized in Fig. 1.

Although the FWHM of the PL spectrum of organic light-emitting materials is wide, the FWHM of the electroluminescence (EL) spectrum of OLED devices can be narrowed by applying a microcavity structure. By applying a cavity effect to enhance the intensity of a specific wavelength and suppress the intensity of other wavelengths, a narrow EL spectrum can be obtained. However, if the FWHM of the PL spectrum is wide, the improved efficiency may be unimpressive even if the cavity effect is applied because the suppressed wavelength regions will be lost. By increasing the horizontal oriented dipole rate (HODR) of the organic light-emitting materials in OLED devices, the luminance can

---
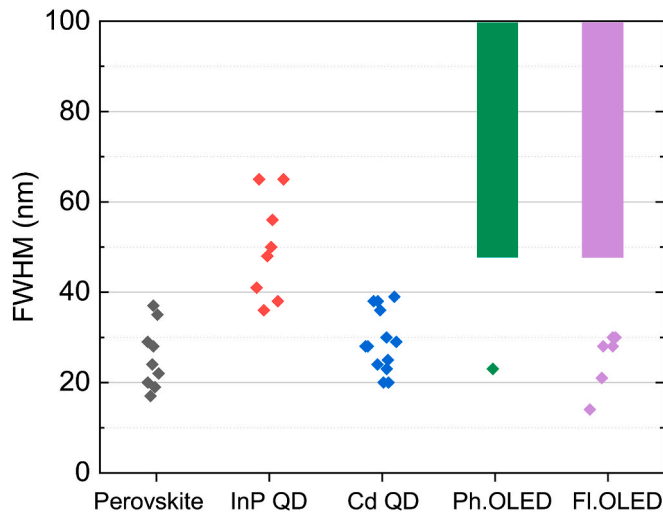
Fig. 1. FWHM of PL spectrum for various light-emitting materials.

Fig. 2. (a) Luminance of top-emitting OLED for different HTL and ETL thicknesses. (b) Emission spectra of top-emitting OLEDs of structures A, B, C, and D.

be compensated and related studies have been widely conducted recently [27–31]. Although light-emitting materials with a narrow FWHM of the PL spectrum, such as a QD or perovskite, has an isotropic orientation, organic light-emitting materials can exhibit various dipole orientations based on the molecular structure and deposition conditions. In this study, we investigate the amount of luminance that can be compensated when using a high HODR while achieving a high color gamut in OLEDs through an optical structure design.

2. Results and discussion

For optical simulation, the commercial software Setfos (FLUXiM AG) was applied. The simulated top-emitting OLED structure comprise a reflective Al bottom electrode, a hole transporting layer (HTL), an emission layer (EML), an electron transporting layer (ETL), a thin layer of Ag for a semitransparent top electrode, and a capping layer (CPL) as shown in the inset in Fig. 2(a). Other functional layers such as a hole injection layer and an electron injection layer can be added to improve the electrical properties, although their thicknesses optically merge into the thickness of the HTL or ETL. The thicknesses of the thin Ag and CPL were fixed at 15 and 60 nm, respectively. The optical constants used for the HTL, ETL, and EML were those of 1,3-Bis[3,5-di(pyridin-3-yl) phenyl]benzene (BmPyPhB), 1,1-bis[(di-4-tolylamino)phenyl]cyclohexane (TAPC), and 2,6-Bis(3-(9H -carbazol-9-yl)phenyl)pyridine (26DCzPPy), respectively (see Fig. S1), whereas those of Ag and Al were obtained from the software.

When the HTL and ETL thicknesses were changed, the luminance is changed significantly owing to a strong cavity effect. The luminance was calculated as shown in Fig. 2(a), assuming that the intensity of the PL spectrum was constant in all visible wavelength regions. Consequently, the luminance was determined by how much it overlapped the photopic response curve. The device structure, where both the HTL and ETL thicknesses correspond to the first cavity length (structure A), has HTL and ETL thicknesses of 50 and 45 nm, respectively. The device structure where the HTL thicknesses correspond to the second cavity length (structure B) has an HTL thickness of 220 nm, whereas the device structure in which the ETL thickness corresponds to the second cavity length (structure C) has an ETL thickness of 190 nm. The device structure where both the HTL and ETL thicknesses correspond to the second cavity length is denoted as structure D.

Fig. 2(b) shows the emission spectra of the device with structures A, B, C, and D. These emission spectra correspond to the cavity enhancement factor $G_{cav}(\lambda)$ because the intensity of the intrinsic PL spectrum is assumed to be unity. This is affected by not only the optical properties of
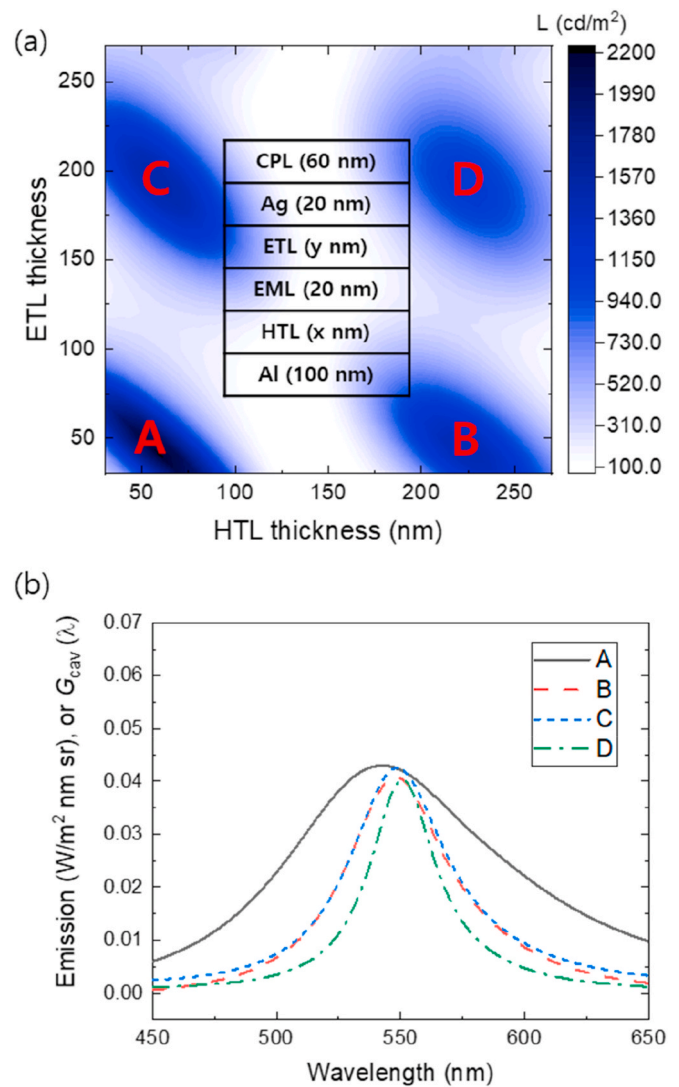
the two electrodes, but also the phase difference, $\Delta\varphi(\lambda)$. $G_{cav}(\lambda)$ and $\Delta\varphi(\lambda)$ are expressed as

$$G_{cav}(\lambda) \propto \frac{T_t\left(1 + \sqrt{R_r}\right)^2}{\left(1 - \sqrt{R_t R_r}\right)^2 + 4\sqrt{R_t R_r}\sin^2\left(\frac{\Delta\varphi(\lambda)}{2}\right)} \tag{1}$$

$$\Delta\varphi(\lambda) = \varphi_m + \Sigma\frac{4\pi nd\cos\theta}{\lambda} \tag{2}$$

where R_t and R_r are the reflectances of the transparent electrode and reflective electrode, respectively, respectively; T_t is the transmittance of the transparent electrode; φ_m is the phase change occurring upon reflection at two electrodes in the OLED structure; n and d are the refractive index and thickness of the organic layers, respectively; θ is the angle of light propagation in each layer [32–34]. As the thickness of the HTL or ETL increases, the FWHM of $G_{cav}(\lambda)$ becomes narrower even for the same electrode structures. The FWHMs of $G_{cav}(\lambda)$ were 104, 50, 49, and 33 nm for structures A, B, C, and D, respectively.

In addition, optimized structures exist for blue and red emission. Fig. 3(a) and (b) show the $G_{cav}(\lambda)$ of the device with structures A, B, C, and D for blue and red emissions, respectively. The thicknesses of the HTL and ETL correspond to the device structures, and emission colors
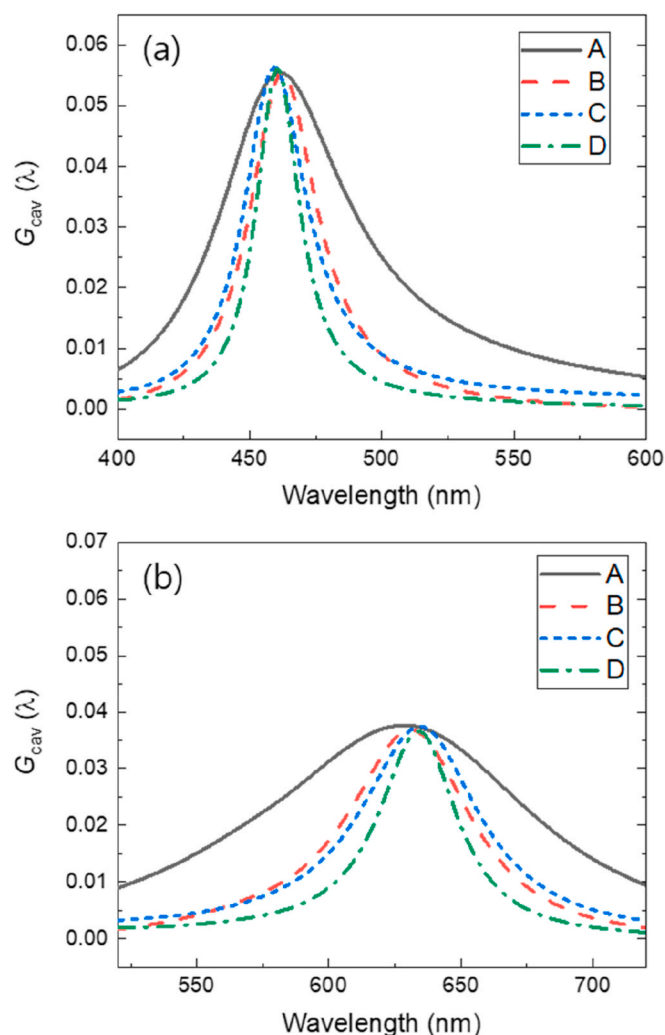
Fig. 3. Cavity enhancement factor ($G_{cav}(\lambda)$) of top-emitting OLEDs of structures A, B, C, and D for (a) blue and (b) red emissions. (For interpretation of the references to color in this figure legend, the reader is referred to the Web version of this article.)

are summarized in Table 1. Not only the ETL and HTL thicknesses but also the FWHM of the $G_{cav}(\lambda)$ varied based on the color. The optimized HTL and ETL thicknesses increased as the emission wavelength shifted to a long wavelength owing to the relationship between λ and d shown in Eq. (2). The FWHM of $G_{cav}(\lambda)$ was narrower in the blue emission than in the green and red emissions owing to the dispersion of the refractive index. The refractive index is a function of wavelength, and the refractive index of an organic material generally decreases as the wavelength increases as shown in Fig. S1. In particular, the change in the refractive index is large in the wavelength region corresponding to blue light emission. Therefore, $\Delta\varphi(\lambda)$ changes significantly as the wavelength changes in blue emission, resulting in a relative narrow FWHM of $G_{cav}(\lambda)$. In addition, R_t in Eq. (1) varies based on the wavelength (see

Fig. S2), thereby affecting on the FWHM of $G_{cav}(\lambda)$ in each color. Because R_t is affected by the thickness and material of the top electrode and the CPL, $G_{cav}(\lambda)$ may vary based on the colors. The FWHM of $G_{cav}(\lambda)$ corresponding to the device structures and emission colors are summarized in Table 1.

Fig. 4a–e show the calculated EL spectra in the device with structure A and B for blue, green, and red emissions, respectively. Various FWHMs of the PL spectrum were used as input parameters in the optical simulation. As shown in Fig. S3(a)–S3(c), the PL spectra exhibited peak wavelengths at 470, 550, and 630 nm for each blue, green, and red emissions, respectively. By changing the FWHM of the PL spectra from 20 to 80 nm, the FWHM of the PL spectra of various emitting materials can be reflected, as shown in Fig. 1. In this study, the EL spectra calculated for the devices with structures C and D were not considered. This is because the FWHMs of $G_{cav}(\lambda)$ for structures B and C are similar, as shown in Table 1. In addition, although structure D had a narrower FWHM of $G_{cav}(\lambda)$ than structure B, the optical effect in the EL spectra owing to this difference was insignificant [35]. Furthermore, intentionally creating structure D may result in electrical issues, such as an increase in driving voltage because the hole mobility of the HTL is a few orders of magnitude greater than the electron mobility of the ETL [36].

Owing to the strong cavity effect of the top-emitting structure, the FWHM of the EL spectrum was smaller than that of the PL spectrum regardless of the device structures and emission color. As mentioned above, the $G_{cav}(\lambda)$ for the blue emission had a narrower FWHM than those of the green and red emissions. Therefore, the blue EL spectra had a narrower FWHM than the green and red EL spectra for the same FWHM of PL spectra and the same structure. The FWHMs of the PL and EL spectra are summarized in Table 2. In the case of blue emission for structure A, when the FWHM of the PL spectrum was 80 nm or less, the FWHM of the EL spectrum became 47 nm or less. Because the FWHM of $G_{cav}(\lambda)$ in structure A is as narrow as 61 nm, even if the FWHM of the PL spectrum is wide, the FWHM of the EL spectrum can be reduced sufficiently. For the green and red emissions, the FWHM of $G_{cav}(\lambda)$ for structure A is wider than 80 nm, as shown in Table 1. If the FWHM of the PL spectrum is wider than 40 nm, then the FWHM of the EL spectrum will be reduced by the cavity effect and wider than 40 nm, which is insufficient for a high color purity. Therefore, in structure A, the use of OLED materials with a wide FWHM of the PL spectrum cannot yield a high color gamut compared with devices using QD materials. If the FWHM of the PL spectrum is narrower than 40 nm, then the FWHM of the EL spectrum is similar to or slightly narrower than that of the PL spectrum.

However, the FWHM of $G_{cav}(\lambda)$ for structure B is narrower than 55 nm as shown in Table 1, indicating that the FWHM of the EL spectrum is less than 29 nm for blue, 41 nm for green, and 44 nm for red emissions. The FWHM of the EL spectrum is similar to that of the QDs-based device. Therefore, although organic light-emitting materials have a wide FWHM of the PL spectrum, OLED devices can have a narrow EL spectrum through a careful optical structure design in which the thickness of either the HTL or ETL is larger than the second cavity length.

It must be confirmed whether the FWHM of the EL spectrum obtained from the top-emitting structure using the EML with a wide FWHM of the PL spectrum is adequate to achieve a high color purity. Fig. 5 shows a CIE 1931 color space chromaticity diagram of an arbitrary white spectrum, which is composed of blue, green, and red colors of various

Table 1
Thicknesses of HTL and ETL, and FWHM of G_{cav} for structures A and B.

Structure	Blue			Green			Red		
	ETL (nm)	HTL (nm)	FWHM of G_{cav} (nm)	ETL (nm)	HTL (nm)	FWHM of G_{cav} (nm)	ETL (nm)	HTL (nm)	FWHM of G_{cav} (nm)
A	35	40	61	45	50	104	60	60	122
B	35	175	31	45	220	50	60	250	55
C	155	40	29	190	50	49	235	60	57
D	155	175	20	190	220	33	235	250	36
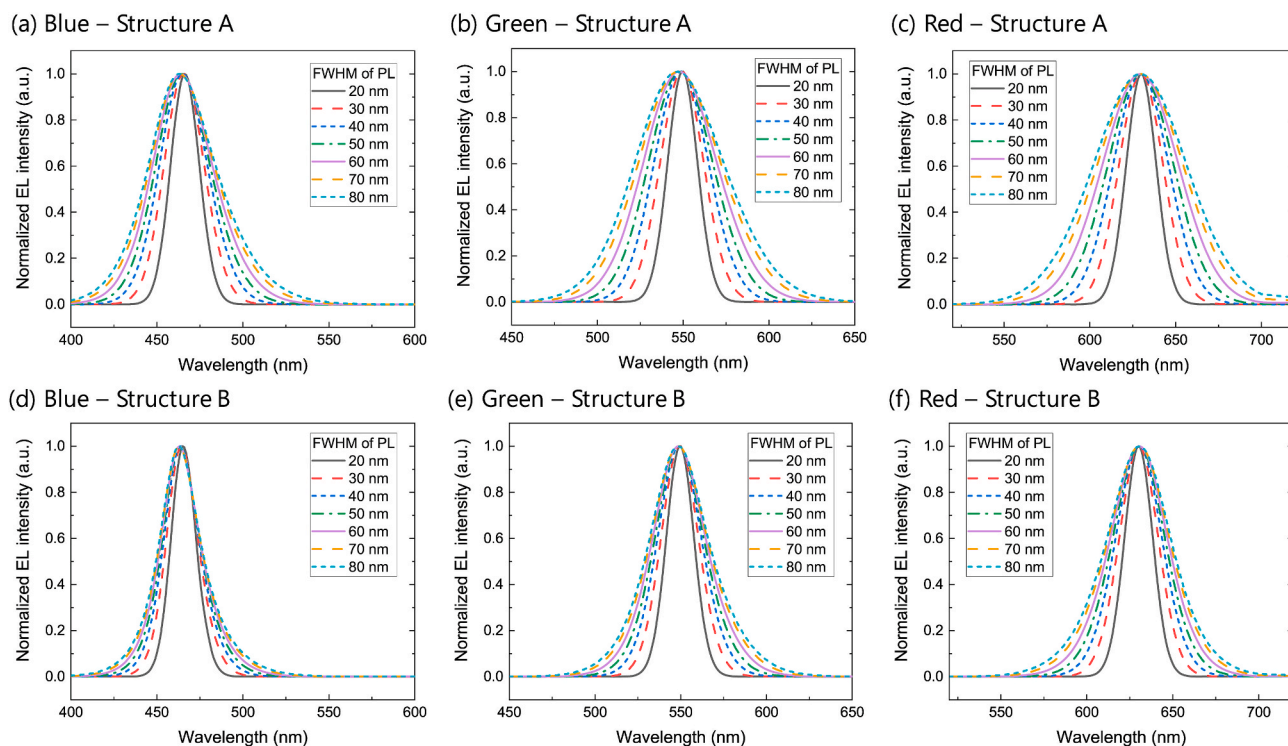
Fig. 4. Calculated EL spectra of top-emitting devices for various FWHM of PL spectrum according to the structure (top row ((a) – (c)): structure A, and bottom row ((d) – (f)): structure B) and color (left column ((a), (d)): blue, middle column ((b), (e)): green, and right column ((c), (f)): red). (For interpretation of the references to color in this figure legend, the reader is referred to the Web version of this article.)

Table 2
FWHM of PL and EL spectra for structures A and B, and emission color.

PL FWHM (nm)			80	70	60	50	40	30	20
EL FWHM (nm)	Blue	A	47	45	41	37	33	28	20
		B	29	28	28	27	24	22	17
	Green	A	61	57	50	44	37	30	20
		B	41	39	37	34	30	26	19
	Red	A	64	59	52	45	38	30	21
		B	44	42	39	36	32	27	19

FWHMs with emission peak positions of 467, 532, and 630 nm, respectively. For example, the inset in Fig. 5 shows a white spectrum with primary colors with a 30-nm FWHM of the EL spectrum, where the color gamut ratio of the BT.2020 standard reached 90% within the CIE color space. The color gamut ratio of the BT.2020 standard for other white spectra having primary colors with different FWHMs are summarized in Table 3. Considering that the FWHM of the EL spectrum is less than 29 nm for blue, 41 nm for green, and 44 nm for red emission in structure B, the OLED devices can achieve over 80% of the color gamut ratio of the BT.2020 standard.

Although the color gamut of the top-emitting devices can be increased through the optical design regardless of the FWHM of the PL spectrum, the luminance must be considered as well. The color coordinate is dominantly determined by the narrower spectrum between $G_{cav}(\lambda)$ of the device and the PL of the light-emitting material. As mentioned previously, the EL spectrum is narrower than the PL spectrum for the device with structure B and the color gamut can be improved significantly. However, the luminance is determined by the product of $G_{cav}(\lambda)$ of the device and the PL spectrum of the light-emitting material. When designing the structure of a top-emitting device with an emitter with a wide FWHM of the PL spectrum, the FWHM of $G_{cav}(\lambda)$ is reduced to increase the color gamut, resulting in a reduction in the overlap between $G_{cav}(\lambda)$ and the PL spectrum. Because the PL spectrum that does not overlap with $G_{cav}(\lambda)$ is the loss, a wide FWHM of the PL
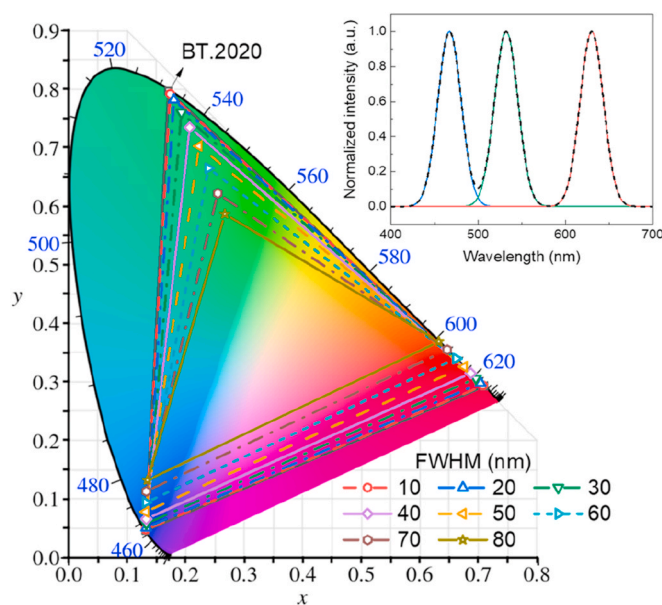
Fig. 5. CIE (x, y) chromaticity coordinates of white spectrum comprising blue, green, and red primary colors with different FWHMs of PL spectra. Inset: white spectrum comprising blue, green, and red primary colors with 30-nm FWHM of PL spectra. (For interpretation of the references to color in this figure legend, the reader is referred to the Web version of this article.)

spectrum is disadvantageous for luminance.

Fig. 6(a)–6(c) show the luminance of the device with structure A for the FWHM of the PL spectrum and the HODR of a light-emitting material. The $G_{cav}(\lambda)$ in structure A is sufficiently wide to encompass the PL spectrum with an FWHM of less than 80 nm. Because the green emission is almost similar to the photopic response curve, it can be explained only

Table 3
Color gamut of white spectra having primary colors with different FWHM.

FWHM (nm)	80	70	60	50	40	30	20	10
Color Gamut[a] (%)	46	55	65	75	83	90	96	99

[a] Ratio of BT.2020 standard.

by the overlap between the PL spectrum and $G_{cav}(\lambda)$. In the normalized PL spectrum, as its FWHM becomes narrower, its peak intensity increases and it overlaps more with the center of $G_{cav}(\lambda)$. Hence, the narrower the FWHM of the PL spectrum, the higher is the luminance. However, in the blue and red emissions, the narrower the FWHM of the EL, the less is the overlap with the photopic response curve, which is disadvantageous for luminance. A trade-off exists between increasing the intensity and decreasing the overlap with the photopic response curve. Therefore, as shown in Fig. 6(a) and 6(c), the luminance of the blue and red emissions do not change significantly even when the FWHM of the PL spectrum narrowed.

Fig. 6(d)–6(f) show the luminance of the device with structure B for the FWHM of the PL spectrum and the HODR of the light-emitting materials. Unlike in structure A, luminance improved in all colors when the FWHM of the PL spectrum narrowed. As shown in Table 2, the FWHM change of the EL spectrum in structure B is much smaller than that in structure A. Consequently, it is more important to improve the peak intensity of the EL spectrum than to overlap with the photopic response curve. To improve the peak intensity of the EL spectrum, the overlap of the $G_{cav}(\lambda)$ and PL spectra must be increased. As the FWHM of the PL spectrum becomes narrower, the luminance improvement becomes greater, as mentioned in a previous paragraph. In addition, because the FWHM of $G_{cav}(\lambda)$ in structure B is less than 55 nm, the luminance improves more when the FWHM of the PL spectrum decreases from 30 nm to 20 nm than when the FWHM of PL decreases from 80 to 70 nm.

Although the luminance characteristics differ for each color according to the structure, structure A is advantageous for luminance. For the same FWHM of the PL spectrum, the luminance in structure A is higher than that in structure B because the $G_{cav}(\lambda)$ in structure A has a similar intensity but a wider FWHM as shown in Figs. 2(b) and 3(a) and 3(b). In the green emission, the luminance by the 40-nm FWHM of the PL spectrum in structure A is higher than that by the 20-nm FWHM of the PL spectrum in structure B. Even in the blue and red emissions, the luminance by the 80-nm FWHM of the PL spectrum in structure A is higher than that by the 20-nm FWHM of the PL spectrum in structure B.

The EML having a narrow FWHM of the PL spectrum, such as QDs, can yield a high color purity and a high luminance in structure A. However, the EML with a wide FWHM of the PL spectrum, such as organic light-emitting materials, must be applied in structure B to obtain a high color purity; this is disadvantageous for luminance. However, a method exists that can increase the luminance additionally by adjusting the dipole orientation of the organic light-emitting material without changing the device structure. The difference in luminance originating from the FWHM of the PL spectrum can be compensated using emitting materials with a horizontally oriented dipole. The luminance can theoretically be improved by 1.5-times the original value in an OLED device with a 100% HODR compared to that with an isotropic oriented dipole ratio (66.7% HODR) without any spectral changes [37]. The HODR required an additional increase in the luminance depending on the colors. For example, when assuming that the device with structure A comprised a QD-based EML with a 40-nm FWHM of the PL spectrum and an isotropic dipole orientation, 1,750, 10,000, and 2,850 cd/m² of luminance were achieved for the blue, green, and red emission, respectively, as shown in Fig. 6(a)–6(c). In this case, the FWHMs of the EL spectrum were 33, 37, and 38 nm for the blue, green, and red emissions, respectively, as shown in Table 2. The FWHM of the PL spectrum and the HODR of the organic light-emitting material required to obtain a color purity and luminance similar to that of the QD-based device differ for each color. For the blue emission, even if the FWHM of PL spectrum is 80 nm, the FWHM of the EL spectrum is narrower than 29 nm, but the luminance is not compensated even when the HODR is 100%. For the green emission, if the FWHM of the PL spectrum is smaller than 60 nm, the FWHM of the EL spectrum is 37 nm or less. In terms of
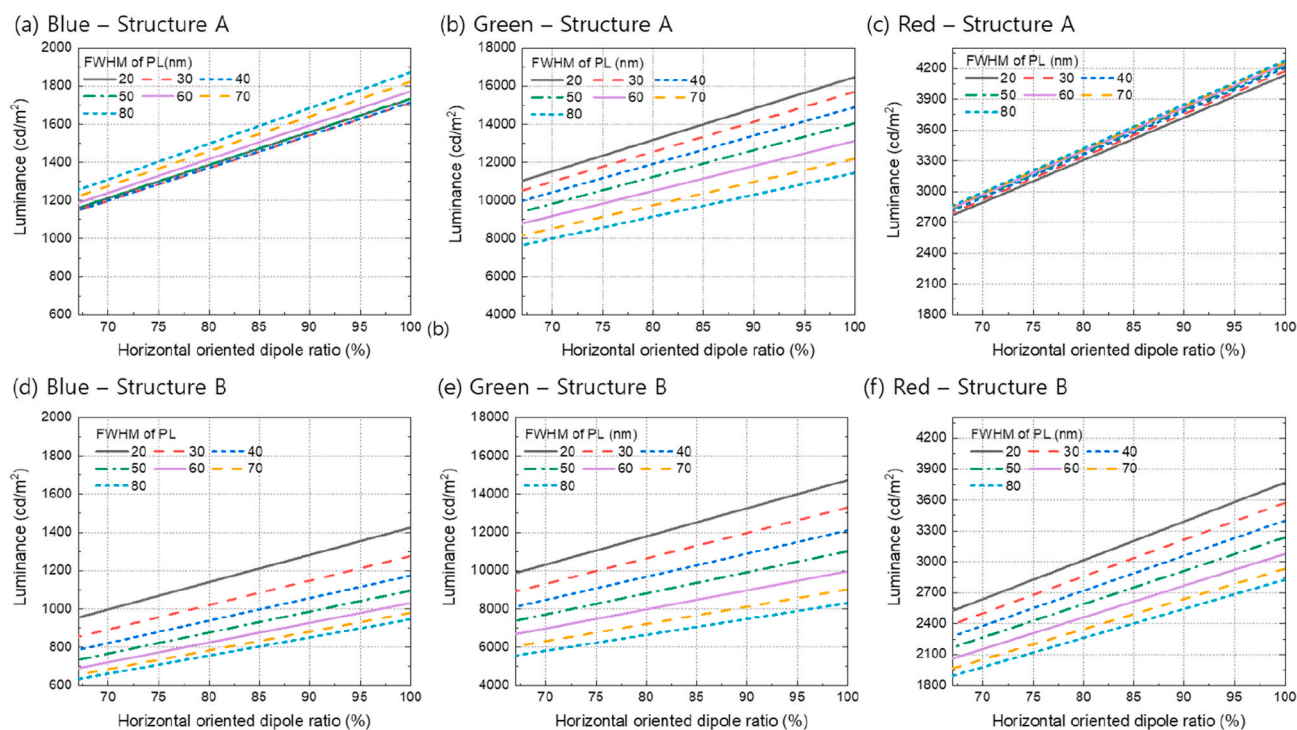
Fig. 6. Luminance based on FWHM of PL spectrum and horizontally oriented dipole ratio of emission layer in top-emitting devices according to the structure (top row ((a) – (c)): structure A, and bottom row ((d) – (f)): structure B) and color (left column ((a), (d)): blue, middle column ((b), (e)): green, and right column ((c), (f)): red). (For interpretation of the references to color in this figure legend, the reader is referred to the Web version of this article.)

luminance compensation, the 60-nm FWHM of the PL spectrum has a 100% HODR to achieve the same luminance, and the 50-nm FWHM of the PL has a 90% or more HODR to achieve a higher luminance. For the red emission, considering the FWHM of the EL spectrum, the FWHM of the PL spectrum should be 60 nm or less, as in the green emission. However, a higher luminance is achieved if the EML has an 83% or more HODR for the 50-nm FWHM of the PL spectrum and an 88% or more HODR for the 60-nm FWHM of the PL spectrum. To further increase the color purity, a structure having a stronger cavity effect, such as structure D, may be applied (see Fig. S4(a)). However, in this case, the luminance reduction is greater; therefore, luminance compensation may not be possible even if a 100% HODR is applied to the case of green emission, as shown in Fig. S4(b).

3. Conclusion

In conclusion, compared with QDs, organic light-emitting materials have a relatively wide PL spectrum, which is disadvantageous for achieving a wide color gamut. Although light-emitting materials with a 70-nm FWHM of the PL spectrum are used, an FWHM of the EL of less than 40 nm can be achieved through the optical design of the device structure, resulting in an 83% color gamut ratio of the BT.2020 standard in the CIE color space. Structurally increasing the color purity in the device with a wide FWHM of the PL spectrum is disadvantageous for luminance. When the horizontal dipole orientation of the organic light-emitting material was applied, the luminance improved without changing the structure. While maintaining a high color purity, the compensation for lower luminance varied depending on the color. The structure for the blue emission had a relatively strong cavity effect. Therefore, a 100% HODR was insufficient to compensate for luminance, and reducing the FWHM of the PL spectrum was effective for fabricating devices with higher efficiency and color purity. For the green and red emissions, although the FWHM of the PL spectrum was 20-nm wider, increasing the HODR yield a similar or higher luminance while maintaining a similar color purity.

Declaration of competing interest

The authors declare that they have no known competing financial interests or personal relationships that could have appeared to influence the work reported in this paper.

Appendix A. Supplementary data

Supplementary data to this article can be found online at https://doi.org/10.1016/j.orgel.2020.105945.

References

[1] ITU-R Recommendation BT.2020, Parameter Values for Ultra-high Definition Television Systems for Production and International Programme Exchange, 2012.

[2] R. Zhu, Z. Luo, H. Chen, Y. Dong, S.-T. Wu, Realizing Rec. 2020 color gamut with quantum dot displays, Opt. Express 23 (2015) 23680–23693.

[3] S. Jang, Y. Lee, M.C. Park, OLED lighting for general lighting applications, SID Symposium Digest of Technical Papers 46 (1) (2015) 661–663.

[4] T. Komoda, N. Ide, K. Varutt, K. Yamae, H. Tsuji, Y. Matsuhisa, High-performance white OLEDs with high color-rendering index for next-generation solid-state lighting, J. SID 19 (11) (2011) 838–846.

[5] T. Fleetham, G. Li, L. Wen, J. Li, "Efficient "pure" blue OLEDs employing tetradentate Pt complexes with a narrow spectral bandwidth, Adv. Mater. 26 (2014) 7116–7121.

[6] H. Fukagawa, T. Oono, Y. Iwasaki, T. Hatakeyama, T. Shimizu, High-efficiency ultrapure green organic light-emitting diodes, Mater. Chem. Front. 2 (2018) 704–709.

[7] Y. Kondo, K. Yoshiura, S. Kitera, H. Nishi, S. Oda, H. Gotoh, Y. Sasada, M. Yanai, T. Hatakeyama, Narrowband deep-blue organic light-emitting diode featuring an organoboron-based emitter, Nat. Photon. 13 (2019) 678–682.

[8] T. Hatakeyama, K. Shiren, K. Nakajima, S. Nomura, S. Nakatsuka, K. Kinoshita, J. Ni, Y. Ono, T. Ikuta, "Ultrapure blue thermally activated delayed fluorescence molecules: efficient HOMO–LUMO separation by the multiple resonance effect, Adv. Mater. 28 (2016) 2777–2781.

[9] Y. Takita, N. Hashimoto, K. Takeda, S. Nomura, S. Uesaka, T. Suzuki, H. Nakashima, S. Seo, S. Yamazaki, Highly efficient deep-blue fluorescent dopant for achieving low-power OLED display satisfying BT.2020 chromaticity, J. SID 26 (2) (2018) 55–63.

[10] H. Kido, T. Yamaguchi, H. Inoue, T. Sasaki, N. Ohsawa, S. Seo, S. Yamazaki, "Novel host–guest system for drastic improvement in the lifetime of a deep-red OLED that satisfies the red chromaticity of the BT.2020 standard, SID Digest 49 (2018) 243–246.

[11] J. Lim, M. Park, W.K. Bae, D. Lee, S. Lee, C. Lee, K. Char, Highly efficient cadmium-free quantum dot light-emitting diodes enabled by the direct formation of excitons within InP@ZnSeS quantum dots, ACS Nano 7 (2013) 9019–9026.

[12] J.P. Park, J.-J. Lee, S.-W. Kim, Highly luminescent InP/GaP/ZnS QDs emitting in the entire color range via a heating up process, Sci. Rep. 6 (2016) 30094.

[13] P. Ramasamy, N. Kim, Y.-S. Kang, O. Ramirez, J.-S. Lee, Tunable, bright, and narrow-band luminescence from colloidal indium phosphide quantum dots, Chem. Mater. 29 (2017) 6893–6899.

[14] H.C. Wang, H. Zhang, H.Y. Chen, H.C. Yeh, M.R. Tseng, R.J. Chung, S. Chen, R. S. Liu, "Cadmium-Free InP/ZnSeS/ZnS heterostructure-based quantum dot light-emitting diodes with a ZnMgO electron transport layer and a brightness of over 10,000 cd m−2, Small 13 (2017) 1603962.

[15] P. Ramasamy, K.-J. Ko, J.-W. Kang, J.-S. Lee, "Two-Step "seed-mediated" synthetic approach to colloidal indium phosphide quantum dots with high-purity photo- and electroluminescence, Chem. Mater. 30 (2018) 3643–3647.

[16] F. Cao, S. Wang, F. Wang, Q. Wu, D. Zhao, X. Yang, "A layer-by-layer growth strategy for large-size InP/ZnSe/ZnS core–shell quantum dots enabling high-efficiency light-emitting diodes, Chem. Mater. 30 (2018) 8002–8007.

[17] Y.-H. Won, O. Cho, T. Kim, D.-Y. Chung, T. Kim, H. Chung, H. Jang, J. Lee, D. Kim, E. Jang, Highly efficient and stable InP/ZnSe/ZnS quantum dot light-emitting diodes, Nature 575 (2019) 634–638.

[18] L. Qian, Y. Zheng, J. Xue, P.H. Holloway, Stable and efficient quantum-dot light-emitting diodes based on solution-processed multilayer structures, Nat. Photon. 5 (2011) 543–548.

[19] X. Dai, Z. Zhang, Y. Jin, Y. Niu, H. Cao, X. Liang, L. Chen, J. Wang, X. Peng, Solution-processed, high-performance light-emitting diodes based on quantum dots, Nature 515 (2014) 96–99.

[20] W.K. Bae, J. Lim, D. Lee, M. Park, H. Lee, J. Kwak, K. Char, C. Lee, S. Lee, R/G/B/ Natural white light thin colloidal quantum dot-based light-emitting devices, Adv. Mater. 26 (2014) 6387–6393.

[21] Y. Yang, Y. Zheng, W. Cao, A. Titov, J. Hyvonen, J.R. Manders, J. Xue, P. H. Holloway, L. Qian, High-efficiency light-emitting devices based on quantum dots with tailored nanostructures, Nat. Photon. 9 (2015) 259–266.

[22] Z.-K. Tan, R.S. Moghaddam, M.L. Lai, P. Docampo, R. Higler, F. Deschler, M. Price, A. Sadhanala, L.M. Pazos, D. Credgington, F. Hanusch, T. Bein, H.J. Snaith, R. H. Friend, Bright light-emitting diodes based on organometal halide perovskite, Nat. Nanotechnol. 9 (2014) 687–692.

[23] J. Wang, N. Wang, Y. Jin, J. Si, Z.-K. Tan, H. Du, L. Cheng, X. Dai, S. Bai, H. He, Z. Ye, M.L. Lai, R.H. Friend, W. Huang, "Interfacial control toward efficient and low-voltage perovskite light-emitting diodes, Adv. Mater. 27 (2015) 2311–2316.

[24] J. Byun, H. Cho, C. Wolf, M. Jang, A. Sadhanala, R.H. Friend, H. Yang, T.-W. Lee, "Efficient visible quasi-2D perovskite light-emitting diodes, Adv. Mater. 28 (2016) 7515–7520.

[25] L. Zhang, X. Yang, Q. Jiang, P. Wang, Z. Yin, X. Zhang, H. Tan, Y. Yang, M. Wei, B. R. Sutherland, E.H. Sargent, J. You, Ultra-bright and highly efficient inorganic based perovskite light-emitting diodes, Nat. Commun. 8 (2017) 15640.

[26] K. Qasim, B. Wang, Y. Zhang, P. Li, Y. Wang, S. Li, S.-T. Lee, L.-S. Liao, W. Lei, Q. Bao, "Solution-Processed extremely efficient multicolor perovskite light-emitting diodes utilizing doped electron transport layer, Adv. Funct. Mater. 27 (2017), 1606874.

[27] T.D. Schmidt, D.S. Setz, M. Flämmich, J. Frischeisen, D. Michaelis, B. C. Krummacher, N. Danz, W. Brütting, Evidence for non-isotropic emitter orientation in a red phosphorescent organic light-emitting diode and its implications for determining the emitter's radiative quantum efficiency, Appl. Phys. Lett. 99 (2011) 163302.

[28] M. Flämmich, J. Frischeisen, D.S. Setz, D. Michaelis, B.C. Krummacher, T. D. Schmidt, W. Brütting, N. Danz, Oriented phosphorescent emitters boost OLED efficiency, Org. Electron. 12 (2011) 1663–1668.

[29] S.-Y. Kim, W.-I. Jeong, C. Mayr, Y.-S. Park, K.-H. Kim, J.-H. Lee, C.-K. Moon, W. Brütting, J.-J. Kim, Organic light-emitting diodes with 30% external quantum efficiency based on a horizontally oriented emitter, Adv. Funct. Mater. 23 (2013) 3896–3900.

[30] K.-H. Kim, J.-L. Liao, S.W. Lee, B. Sim, C.-K. Moon, G.-H. Lee, H.J. Kim, Y. Chi, J.-J. Kim, Crystal organic light-emitting diodes with perfectly oriented non-doped Pt-based emitting layer, Adv. Mater. 28 (2016) 2526–2532.

[31] T. Komino, Y. Sagara, H. Tanaka, Y. Oki, N. Nakamura, H. Fujimoto, C. Adachi, Electroluminescence from completely horizontally oriented dye molecules, Appl. Phys. Lett. 108 (2016), 241106.

[32] H. Cho, C. Yun, S. Yoo, Multilayer transparent electrode for organic light-emitting diodes: tuning its optical characteristics, Opt. Express 18 (4) (2010) 3404–3414.

[33] H. Cho, J.-W. Shin, N.S. Cho, J. Moon, J.-H. Han, Y.-D. Kwon, S. Cho, J.-I. Lee, Optical effects of graphene electrodes on organic light-emitting diodes, IEEE J. Sel. Top. Quant. Electron. 22 (1) (2016), 2000206.

[34] H. Cho, J. Song, B.-H. Kwon, S. Choi, H. Lee, C.W. Joo, S.-D. Ahn, S.-Y. Kang, S. Yoo, J. Moon, Stabilizing color shift of tandem white organic light-emitting diodes, J. Ind. Eng. Chem. 69 (2019) 414–421.

[35] M.J. Park, Y.H. Son, G.H. Kim, R. Lampande, H.W. Bae, R. Pode, Y.K. Lee, W. J. Song, J.H. Kwon, Device performances of third order micro-cavity green top-emitting organic light emitting diodes, Org. Electron. 26 (2015) 458–463.

[36] Shahnawaz, S.S. Swayamprabha, M.R. Nagar, R.A.K. Yadav, S. Gull, D.K. Dubey, J. H. Jou, Hole-transporting materials for organic light-emitting diodes: an overview, J. Mater. Chem. C 7 (2019) 7144–7158.

[37] H. Cho, C.W. Joo, B.-H. Kwon, N.S. Cho, J. Lee, Non-linear relation between emissive dipole orientation and forward luminous efficiency of top-emitting organic light-emitting diodes, Org. Electron. 62 (2018) 72–76.